

# Photocatalytic decolorization and degradation of Congo Red on innovative crosslinked chitosan/nano-CdS composite catalyst under visible light irradiation

Huayue Zhu<sup>a,b</sup>, Ru Jiang<sup>a,c,\*</sup>, Ling Xiao<sup>b</sup>, Yuhua Chang<sup>b</sup>, Yujiang Guan<sup>a</sup>, Xiaodong Li<sup>c</sup>, Guangming Zeng<sup>c</sup>

<sup>a</sup> Department of Environmental Engineering, Taizhou University, Linhai 317000, PR China

<sup>b</sup> College of Resource and Environmental Science, Wuhan University, Wuhan 430072, PR China

<sup>c</sup> College of Environmental Science and Engineering, Hunan University, Changsha 410082, PR China

## ARTICLE INFO

### Article history:

Received 19 December 2008

Received in revised form 9 April 2009

Accepted 9 April 2009

Available online 18 April 2009

### Keywords:

Chitosan

Nano-CdS

Visible light photocatalysis

Congo Red

Kinetics

## ABSTRACT

The crosslinked chitosan/nano-CdS (CS/n-CdS) composite catalyst prepared by simulating bio-mineralization process was extensively characterized by FT-IR spectra, XRD, SEM, TEM and TGA. An azo dye, Congo Red (CR), was used as model pollutant to study its photocatalytic activity under visible light irradiation. The influences of catalyst amount, initial CR concentrations, pH of the reaction solution and different anions on CR decolorization and degradation reaction kinetics were investigated. Results of characterization indicated the successful formation of hexagonal phase of CdS on raw chitosan under mild conditions. The photocatalytic degradation was found to follow a pseudo-first-order kinetics according to Langmuir–Hinshelwood (L–H) model. The dye could be decolorized more efficiently in acidic media than alkaline media. The presence of  $\text{NO}_3^-$  accelerated evidently the degradation of CR, while the other chosen anions ( $\text{Br}^-$ ,  $\text{SO}_4^{2-}$  and  $\text{Cl}^-$ ) had an inhibitory effect on the decolorization of CR, of which the inhibitory effect of  $\text{Cl}^-$  was the most pronounced. UV–vis spectra were analyzed to indicate that degradation of CR in the solution was the break up of the N=N bonds and degradation of aromatic fragment in this reaction system. The recycling experiments confirmed the relative stability of the catalyst.

© 2009 Elsevier B.V. All rights reserved.

## 1. Introduction

Estimates indicate that approximately 1–15% of the synthetic textile dyes used is lost in wastewater streams during manufacturing or processing operations [1,2]. The discharge of highly colored waste is not only aesthetically displeasing, but it also impedes light penetration, thus upsetting biological processes within a stream. In addition, many dyes are toxic to some organisms and may cause direct destruction of aquatic communities. Hence, removal of dyes from such wastewaters is a major environmental problem and complete dye removal is necessary because dyes will be visible even at low concentrations [3]. Due to the large variability in composition of textile wastewater and the relative stability of dye molecular structures, most of the conventional physicochemical and biological treatment methods are inadequate for their effective removal [4–6]. Advanced oxidation processes (AOPs) are attractive alternatives to non-destructive physical water treatment processes, because they

are able to mineralize organic water contaminants. Among AOPs, one of the most efficient and economical methods is probably the photocatalysis under visible light irradiation because most of the solar spectra fall in the visible range [7–9].

CdS is a well-known semiconductor with a band gap of 2.42 eV and its valence electron can be easily evoked to conduction band when the wavelength of evoking light is less than or equal to 495 nm [10,11]. CdS semiconductor nanoparticles as photocatalyst have attracted intense interest to treat dyes wastewater due to their unique photochemical and photophysical properties in recent years [12,13]. Mechanistically, CdS photocatalyst is first evoked by relevant light and subsequently initiates the photodegradation of contaminants. At first, CdS photocatalyst is first evoked by relevant light to create electrons. The electrons are then scavenged by molecular oxygen  $\text{O}_2$  to yield the superoxide radical anion  $\text{O}_2^{\bullet-}$  (Eq. (2)) and hydrogen peroxide  $\text{H}_2\text{O}_2$  (Eq. (3)) in oxygen-equilibrated media. These new formed intermediates can interreact to produce hydroxyl radical  $\bullet\text{OH}$  (Eq. (4)). It is well known that the  $\bullet\text{OH}$  radical is a powerful oxidizing agent capable of degrading most pollutants (Eq. (5)) [14]:



\* Corresponding author at: No. 605, Dongfang Avenue, Linhai City, Zhejiang Province, 317000, PR China. Tel.: +86 158 67636396; fax: +86 576 85137066.

E-mail addresses: [zhuhuayue@126.com](mailto:zhuhuayue@126.com) (H. Zhu), [jiangru0576@163.com](mailto:jiangru0576@163.com), [jiangru@tzc.edu.cn](mailto:jiangru@tzc.edu.cn) (R. Jiang), [xl9119@public.wh.hb.cn](mailto:xl9119@public.wh.hb.cn) (L. Xiao), [changyuhua1122@126.com](mailto:changyuhua1122@126.com) (Y. Chang), [guanyujiang@tzc.edu.cn](mailto:guanyujiang@tzc.edu.cn) (Y. Guan), [lxdfx@163.com](mailto:lxdfx@163.com) (X. Li), [zgming@hnu.cn](mailto:zgming@hnu.cn) (G. Zeng).

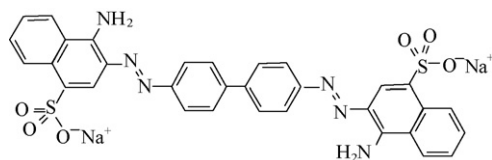
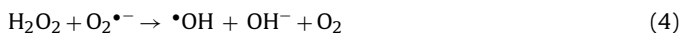


Fig. 1. Chemical structure of Congo Red.



However, CdS nanoparticles are easily to aggregation in aqueous solution during preparation process, which accordingly results in rather lower efficiency. In addition, as powdery catalyst, there are still other limitations such as the difficulty in recycle and reuse.

Some recent literature references have revealed that natural polysaccharide plays an important role in the biosynthesis of nano-sized semiconductor sulfide [15]. The use of natural organic materials in the synthesis of nano-sized material provides an interface for the charge transfer resulting in the increase of photocatalytic efficiency [16]. Chitosan ( $\beta$ -(1  $\rightarrow$  4)-2-amino-2-deoxy-D-glucose, CS) is a natural hydrophilic and cationic polymer product by N-deacetylation of chitin, the next most abundant natural polysaccharide after cellulose [17]. Chitosan has excellent properties for the adsorption of metal ions [18,19], principally due to the presence of high content of amino groups ( $-\text{NH}_2$ ) and hydroxyl ( $-\text{OH}$ ) in the polymer matrix, which makes it a suitable matrix to synthesis semiconductor quantum dots (QDs) and semiconductor composite catalyst [20,21]. Besides, a large number of studies have shown that catalyst or absorbent can be effectively separated and reused if catalyst was immobilized on chitosan [22].

In this present study, the crosslinked chitosan/nano-CdS (CS/n-CdS) composite catalyst was prepared by simulating biomineralization process and characterized in detail. Next, Congo Red (CR) with complex aromatic chemical structure was selected as object pollutant to examine the photocatalytic efficiency of the innovative catalyst for organic dye pollutants. Different factors on the reactive rate were investigated and the kinetic behaviors of reaction were evaluated for CR. The results obtained from this study could provide fundamental information for the design and operation of such a process for the treatment of azo-dye-contaminated industrial effluents.

## 2. Experimental

### 2.1. Materials

Commercially available Congo Red ( $\text{C}_{32}\text{H}_{22}\text{N}_6\text{O}_6\text{S}_2\text{Na}_2$ , C.I. Direct Red 28) was purchased from Yongjia Fine Chemical Factory (Zhejiang, China) and used as received without further purification. Fig. 1 displays the chemical structure of the dye. Samples of chitosan with 92% of deacetylation degree prepared from shrimp shell were purchased from Yuhuan Ocean Biochemical Co., Ltd. (Zhejiang, China).  $\text{CdCl}_2$ ,  $(\text{NH}_2)_2\text{CS}$ ,  $\text{OHC}(\text{CH}_2)_3\text{CHO}$  (25%, v/v),  $\text{NaOH}$ ,  $\text{Na}_2\text{SO}_4$ ,  $\text{NaNO}_3$ ,  $\text{NaCl}$ ,  $\text{NaBr}$ ,  $\text{HNO}_3$  and  $\text{H}_2\text{SO}_4$  were of analytical grade from Shanghai Chemical Reagent Co., Ltd. (Shanghai, China). All the solutions were prepared by double distilled water.  $0.1 \text{ mol L}^{-1}$   $\text{NaOH}$  or  $0.1 \text{ mol L}^{-1}$   $\text{H}_2\text{SO}_4$  in proper amounts was used to adjust the suitable pH value.

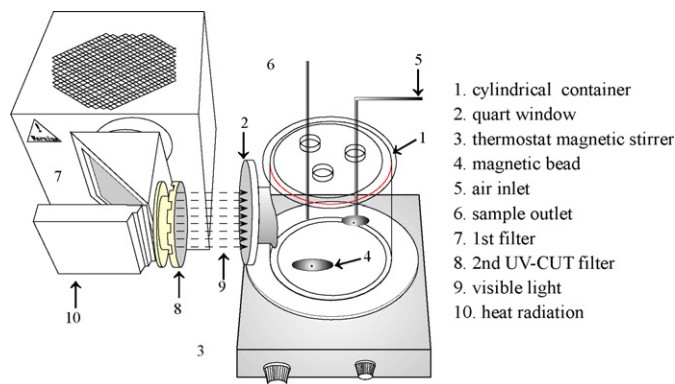


Fig. 2. Schematic diagram of photocatalytic reaction system.

### 2.2. Methods

#### 2.2.1. Preparation of CS/n-CdS composite catalyst

CS/n-CdS composite catalyst was synthesized by simulating biomineralization technique modified from previous literature reports [21]: at room temperature, a 1.5 g amount of chitosan mixed with a 0.9 g amount of  $\text{CdCl}_2$  was dissolved in 120 mL 1% (v/v)  $\text{HNO}_3$  aqueous solution under continuous stirring for 4 h to facilitate a chelating balance. Chitosan complexes with  $\text{Cd}^{2+}$  ions were formed through the adsorption and chelation between chitosan and  $\text{Cd}^{2+}$  ions. The resulting sol solution was kept in water bath at  $60^\circ\text{C}$  for 1 h, in which fresh sulfocarbamide solution was dropped slowly.  $\text{Cd}^{2+}$  ions in chitosan/ $\text{Cd}^{2+}$  complexes reacted with  $\text{S}^{2-}$  released slowly from fresh sulfocarbamide to form chitosan/nano-CdS (CS/n-CdS). Subsequently, in order to stabilize CS/n-CdS in acid solution, the CS/n-CdS was dipped into 100 mL 0.25% glutaraldehyde solution in a 250 mL flash and agitated for 30 min for crosslinking. Crosslinking of chitosan in CS/n-CdS by means of the Schiff's reaction is accomplished when amine functional groups from two monomers of different chitosan chains react with glutaraldehyde [23]. Then 200 mL  $0.1 \text{ mol L}^{-1}$   $\text{NaOH}$  solution was added. The orange yellow end product was filtered and washed with absolute ethyl alcohol and double distilled water, respectively, for 3–4 times. Finally, the product (CS/n-CdS) was dried at  $60^\circ\text{C}$  under atmospheric condition.

#### 2.2.2. Physicochemical characterization of CS/n-CdS composite catalyst

The Fourier transform infrared (FT-IR) spectra were recorded within KBr pellet on a FTIR-8400 spectrometer (Shimadzu, Japan). The X-ray diffraction (XRD) spectra of chitosan and CS/CdS NPs were performed using a D8 ADVANCE X-ray diffraction spectrometer (Bruker, German) with a  $\text{Cu K}\alpha$  target at 40 kV and 50 mA at a scan rate of  $0.02^\circ 2\theta \text{ s}^{-1}$ . The morphological structure of the photocatalyst was examined by scanning electron microscopy (SEM) with a Hitachi SX-650 machine (Tokyo, Japan) and transmission electron microscopy (TEM) with model JEOL-JCM-5700 machine (Tokyo, Japan). Thermogravimetry (TG) was performed using a Setaram Setsys 16 TG/DTA/DSC (France) under a nitrogen atmosphere of 0.15 MPa from 25 to  $800^\circ\text{C}$  with heating rate of  $2^\circ\text{C}/\text{min}$ .

#### 2.2.3. Photodegradation and analysis of Congo Red

Fig. 2 schematically shows the photocatalytic reaction system. Photocatalytic experiments were carried out in a cylindrical organic glass container of dimensions (200 mm diameter, 250 mm height). A 300 W xenon lamp (PLS-SXE300, Beijing Trusttech Co. Ltd., China) loaded with a UV-Cut filter was used as simulated visible light sources to irradiate horizontally into the photocatalytic reactor. A 500 mL of Congo Red solution was mixed with a certain amount of

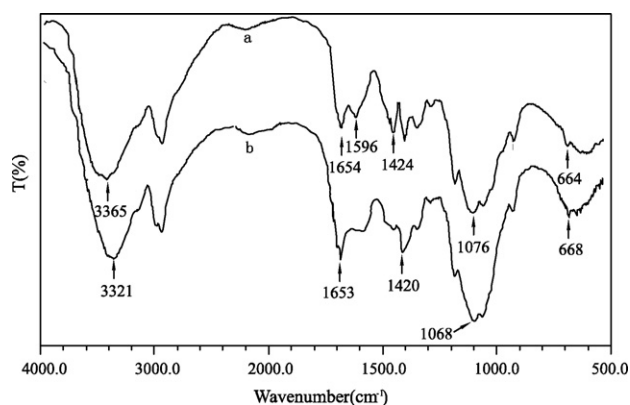


Fig. 3. FT-IR spectra of chitosan (a) and CS/n-CdS (b).

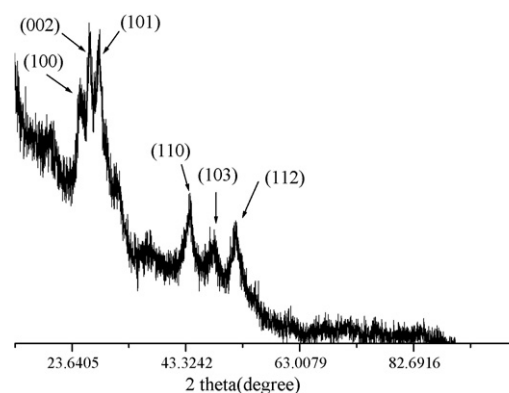


Fig. 4. XRD spectra of CS/n-CdS.

photocatalyst and exposed to the visible light. At given irradiation time intervals, 4 mL of the suspensions were collected, then centrifuged and filtered through a Millipore filter (pore size, 0.22  $\mu\text{m}$ ) to separate the photocatalyst particles. The Millipore filter was washed using double distilled water every time to ensure that no residual dye and catalyst remained on the microfilter. The CR concentration was measured by Cary 50 Model UV-Visible Spectrophotometer (Varian, USA) scanning from 200 nm to 800 nm and the wavelength of maximum absorption at  $\lambda_{\text{max}} = 496.03$  nm was monitored. A calibration plot based on Beer–Lambert's law was established by relating the absorbance to the concentration.

The decolorization and degradation reaction kinetics were studied by varying different parameters such as catalyst amount ([Cata.]), initial concentration of dye ( $[C_0]$ ), pH of the solution and different inorganic anions. Degradation rate was calculated using the following equation

$$\text{Degradation rate (\%)} = \left( \frac{1 - C_i}{C_0} \right) \times 100$$

where  $C_0$  is the initial concentration of CR ( $\text{mg L}^{-1}$ ) and  $C_i$  is the instant concentration in the sample at time  $t$  ( $\text{mg L}^{-1}$ ).

Photocatalytic reactions kinetics on photocatalyst can be expressed by the Langmuir–Hinshelwood (L–H) model [24,25]. When the initial concentration of dye is lower, the reaction rate can be expressed as [26]:

$$\ln \left( \frac{C_i}{C_0} \right) = -k_{\text{app}} t$$

where  $k_{\text{app}}$  is the apparent pseudo-first-order reaction rate constant and  $t$  is the reaction time. A plot of  $\ln(C_i/C_0)$  versus  $t$  will yield a slope of  $-k_{\text{app}}$ .

Adsorption tests in dark were carried out in order to evaluate the adsorption of dye on catalyst surface.

### 3. Results and discussion

#### 3.1. Physicochemical characterization

##### 3.1.1. FT-IR

In order to examine the differences between CS/n-CdS and pure chitosan, the FT-IR spectra were applied to the study. The FT-IR spectrum of CS/n-CdS (trace b in Fig. 3) exhibited many alterations from that of pure chitosan (trace a in Fig. 3). The major differences were: the wide peak at  $3365 \text{ cm}^{-1}$ , corresponding to the stretching vibration of hydroxyl, amino and amide groups, moved noticeably to lower wave numbers ( $3321 \text{ cm}^{-1}$ ) and became broader and stronger, which indicated the strong interaction between these groups and CdS [21]. The FT-IR spectrum of chitosan itself showed

some features of amide groups: amide I and amide II bands at  $1654$  and  $1596 \text{ cm}^{-1}$ , respectively [27]. While the spectrum of CS/n-CdS displayed a disappearance of the band at  $1596 \text{ cm}^{-1}$  and the buildup of the band at  $1654 \text{ cm}^{-1}$ , which maybe was related to the consumption of  $-\text{NH}_2$  groups by glutaraldehyde, as a result of the crosslinking process and the complexation [28]. This consumption can be confirmed by the decrease of the band related to primary  $-\text{NH}_2$  groups at  $1424 \text{ cm}^{-1}$ . As we can observe in Fig. 3, the peak located at  $1076 \text{ cm}^{-1}$  assigned to  $\text{C}_3\text{--O}$  stretching shifted to lower wave number  $1068 \text{ cm}^{-1}$ .

##### 3.1.2. XRD

XRD method was also employed to investigate the formation of CS/n-CdS composite (Fig. 4). Major diffraction peaks (1 0 0), (0 0 2), (1 0 1), (1 1 0), (1 0 3) and (1 1 2) correspond to the hexagonal phase according to CdS (JCPDS 06-0314) [29], which revealed the successful formation of hexagonal phase of CdS on chitosan by simulating bio-mineralization. The average size of the crystalline structure of CS/n-CdS calculated by the analysis of XRD data of (1 1 0), (1 0 2) and (1 0 3) was approximately 23–29 nm according to the Scherrer's formula, that is:

$$D = \frac{\kappa \lambda}{\beta \cos \theta}$$

where  $D$  is the crystal size (nm),  $\lambda$  is the Cu  $K\alpha$  wavelength (0.15406),  $\beta$  is half-width of the peak in radians and  $\theta$  is the corresponding diffraction angle [14].

##### 3.1.3. SEM and TEM

The direct evidence of the formation of nanoparticles on the surface of chitosan was given by SEM (Fig. 5a) and TEM (Fig. 5b). In Fig. 5a, there existed many pleats on the surface of CS/n-CdS, which could provide a much larger surface area for photocatalytic reaction. The CS/n-CdS had a spherical morphology with about diameters of 25–35 nm in the TEM image (Fig. 5b), which was in close agreement with XRD data.

##### 3.1.4. TGA

Thermal stabilities of the pure chitosan, crosslinked chitosan film and CS/n-CdS were measured using thermal gravimetric analysis (Fig. 6). The TG curve of CS/n-CdS was very different from that of pure chitosan. The pure chitosan exhibited a weight loss starting at about  $21^\circ\text{C}$  and a rapid weight loss at  $290\text{--}430^\circ\text{C}$ . When the temperature was above  $500^\circ\text{C}$ , chitosan was decomposed slowly and the total weight loss was about 66.0% at  $800^\circ\text{C}$ . However, the tendency of the TGA curve of CS/n-CdS was similar to that of crosslinked chitosan film. There were three steps (at  $20\text{--}250^\circ\text{C}$ ,  $250\text{--}500^\circ\text{C}$ , and  $500\text{--}800^\circ\text{C}$ , respectively) in the TGA curves of both CS/n-CdS and crosslinked chitosan film. The first stage ranges

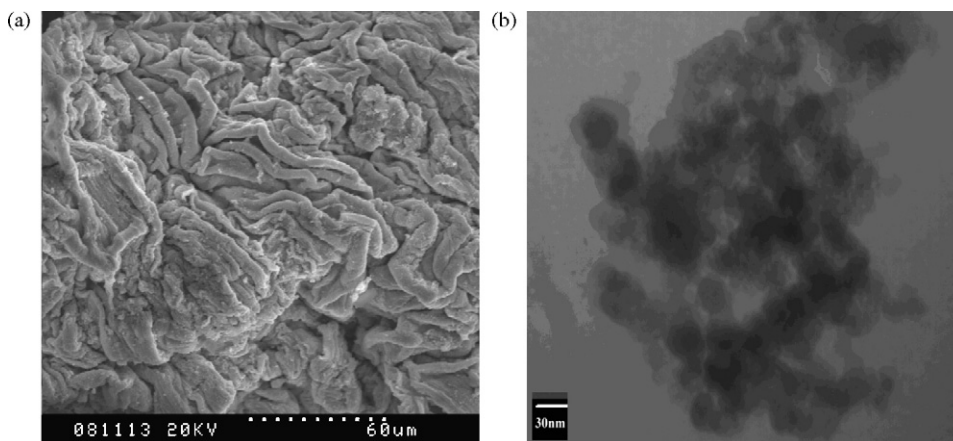


Fig. 5. SEM micrographs (a) and TEM micrographs (b) of representative CS/n-CdS.

showed about 9% weight loss of CS/n-CdS took place, which may be related to the loss of adsorbed and bound water [30]. The other two steps at 250–500 °C and 500–800 °C were caused by the decomposition of residual organic group. The total weight loss of CS/n-CdS by 800 °C was more about 7% than that of crosslinked chitosan films, and excess residual components were mostly CdS. It can be concluded that CS/n-CdS composite exhibited better thermal stability than did the pure chitosan.

### 3.2. Decolorization and degradation of Congo Red in different systems

Fig. 7 shows the decolorization of the CR dye using three different treatment processes, that is under only simulated visible light (trace a), in the presence of CS/n-CdS ( $1.5 \text{ g L}^{-1}$ ) in dark (trace b) and in the presence of CS/n-CdS ( $1.5 \text{ g L}^{-1}$ ) under simulated visible light irradiation (trace c), respectively. For blank experiments in the absence of the catalyst under simulated visible light, almost no degradation of the dye took place. In the presence of CS/n-CdS, but without irradiation, only 20.4% decolorization was observed within 180 min due to the adsorption of the dye and the amount of adsorbed dye was  $2.72 \text{ mg dye/g catalyst}$ . However, when the dye solution in the presence of CS/n-CdS was exposed to the same simulated visible light irradiation within 180 min, about 85.9% of the dye was decolorized and degraded. The UV-vis spectra of the original CR solution and the degraded dye solutions using three different treatment processes after 180 min are presented in Fig. 8. The full spectrum scanning pattern showed extremely obvious difference

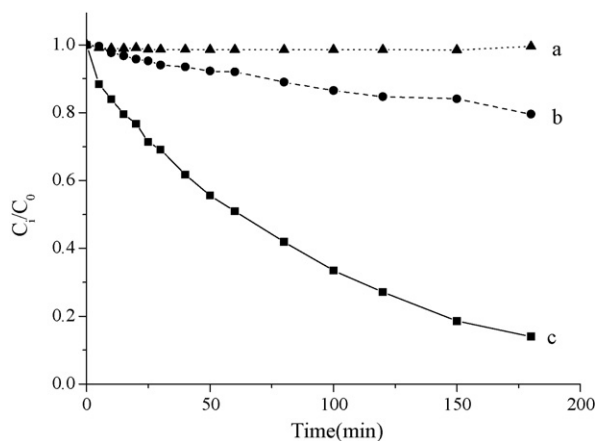


Fig. 7. Comparison of change in concentration as a function of irradiation time: (a) only simulated visible light; (b) CS/n-CdS catalyst ( $1.5 \text{ g L}^{-1}$ ) in dark; (c) CS/n-CdS catalyst ( $1.5 \text{ g L}^{-1}$ ) under simulated visible light irradiation.

after 180 min for three different processes. No peak was detected in the analyzed wavelength range at the end of the 180 min of reaction time in the presence of CS/n-CdS ( $1.5 \text{ g L}^{-1}$ ) under simulated visible light irradiation (trace d in Fig. 8). As a result, both catalyst and an appropriate light source are necessary for photocatalytic decolorization and degradation of the CR dye on innovative CS/n-CdS composite to occur.

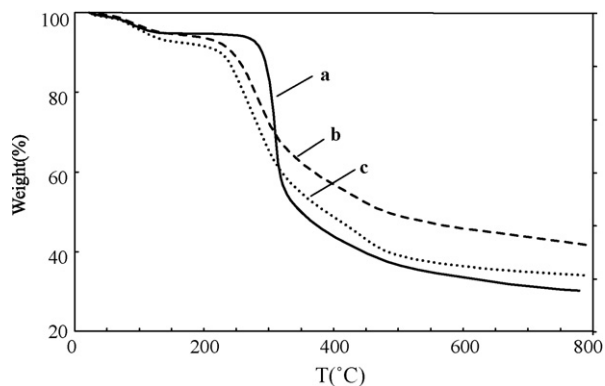


Fig. 6. Thermal gravimetric curves of pure chitosan (a), CS/n-CdS (b), and crosslinked chitosan film (c).

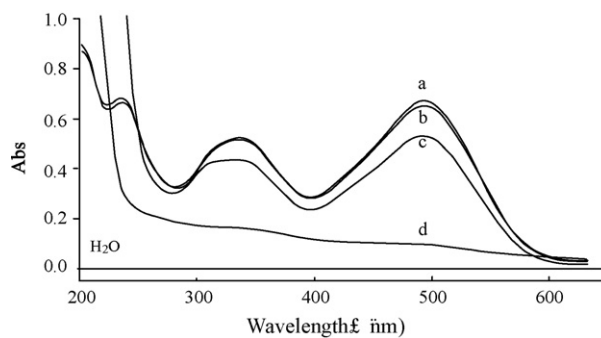
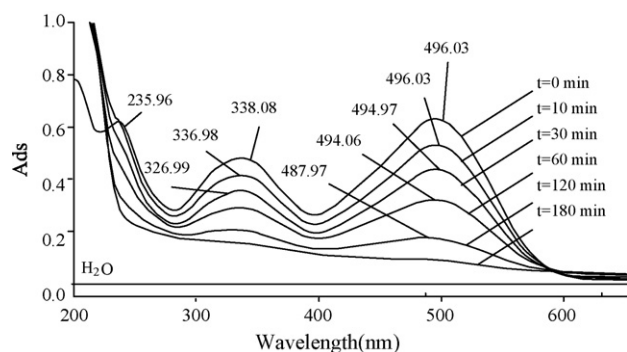


Fig. 8. UV-vis spectra of azo CR solutions and the degraded dye solutions under different conditions at 180 min: (a) original solution; (b) only simulated visible light; (c) CS/n-CdS catalyst ( $1.5 \text{ g L}^{-1}$ ) in dark; (d) CS/n-CdS catalyst ( $1.5 \text{ g L}^{-1}$ ) under simulated visible light irradiation.



**Fig. 9.** UV-vis spectral changes with reaction time.  $[C]_0 = 20 \text{ mg L}^{-1}$ ,  $[Cata.] = 1.5 \text{ g L}^{-1}$ , pH 6.0.

### 3.3. Decolorization and aromatic ring destruction of photocatalytic reaction

To clarify the changes of molecular and structural characteristics of CR as a result of photocatalytic degradation, representative UV-vis spectra changes of the dye solution as a function of reaction time are depicted in Fig. 9. As observed from Fig. 9, absorption spectrum of the original  $20 \text{ mg L}^{-1}$  CR solution was characterized by one main band in the visible region with its maximum absorption at  $496.03 \text{ nm}$  and by other two bands in the ultraviolet region located at  $235.96 \text{ nm}$  and  $338.08 \text{ nm}$ , respectively. The absorbance peaks at  $235.96 \text{ nm}$  and  $338.08 \text{ nm}$  were attributed to “benzene, naphthalene rings” structures, while the absorbance peak at  $496.03 \text{ nm}$  was attributed to the azo bonds of CR molecule [31]. During photodegradation the absorbance values diminish and no more specific peaks at  $496.03 \text{ nm}$  remain after 180 min of reaction, which was due to the fragmentation of the azo links by attack. In addition to this effective bleaching effect, the decay of the absorbance at  $235.96 \text{ nm}$  and  $338.08 \text{ nm}$  were considered as evidence of aromatic fragment degradation in the dye molecule and its intermediates.

The abatement rates of the three absorption peaks ( $235.96 \text{ nm}$ ,  $338.08 \text{ nm}$  and  $496.03 \text{ nm}$ ) in the presence of CS/n-CdS ( $1.5 \text{ g L}^{-1}$ ) composite catalyst under simulated visible light irradiation could be compared conveniently in terms of first-order rate constants [32,33], obtained from the slopes of plots in Fig. 10. The significantly faster rate ( $k_{app} = 11.08 \times 10^{-3} \text{ min}^{-1}$ ) of decay of the visible band was attributed to the priority of cleavage of the azo links in the photocatalytic decolorization and degradation, resulting in the rapid disappearance of chromophores in the dye structure. The result

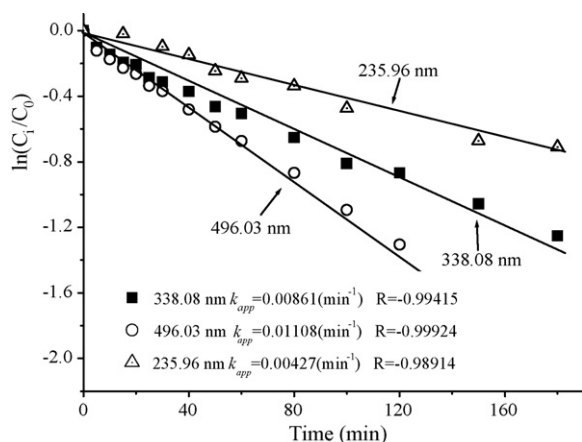


**Fig. 10.** The degradation kinetics of three absorption peaks of CR with reaction time.  $[C]_0 = 20 \text{ mg L}^{-1}$ ,  $[Cata.] = 1.5 \text{ g L}^{-1}$ , pH 6.0.

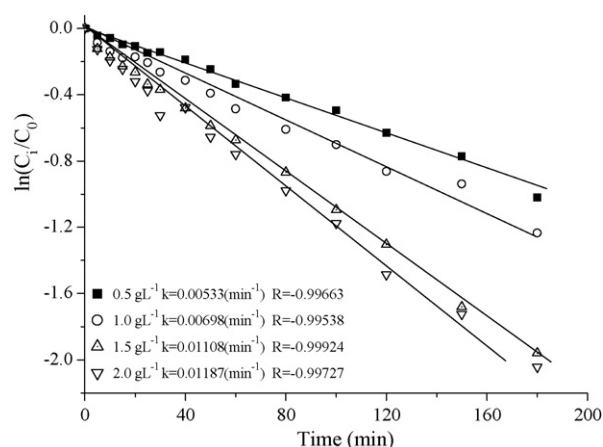


**Fig. 11.** Influence of catalyst amount on the decolorization kinetics of CR.  $[C]_0 = 20 \text{ mg L}^{-1}$ , pH 6.0.

indicated that the break up of the  $\text{N}=\text{N}$  bonds, responsible for the coloration of the azo compounds, was the first step of the oxidative process. Additionally, the  $k_{app}$  value at  $235.96 \text{ nm}$  and at  $338.08 \text{ nm}$  were  $4.27 \times 10^{-3} \text{ min}^{-1}$  and  $8.61 \times 10^{-3} \text{ min}^{-1}$ , respectively, which indicated that “benzene-like” structures and naphthalene ring of CR were also deconstructed to a certain extent during photocatalytic reaction. Therefore, we can conclude that not only decolorization but also degradation of CR took place on innovative CS/n-CdS composite catalyst under visible light irradiation.

### 3.4. The effect of catalyst amount on the decolorization of Congo Red

The effect of photocatalyst amount on decolorization kinetics of the model compound was studied by varying from  $0.5$  to  $2 \text{ g L}^{-1}$ . As seen in Fig. 11, the  $k_{app}$  values increased evidently from  $5.33 \times 10^{-3} \text{ min}^{-1}$  to  $11.08 \times 10^{-3} \text{ min}^{-1}$  with the increase in catalyst amount at the range from  $0.5 \text{ g L}^{-1}$  to  $1.5 \text{ g L}^{-1}$ . This was due to the increase in the catalyst amount, which contributed to the increase in the number of photons adsorbed and also the number of the dye molecules adsorbed. However, catalyst amount further increased up to  $2.0 \text{ g L}^{-1}$  led to the  $k_{app}$  value increased slowly up to  $11.87 \times 10^{-3} \text{ min}^{-1}$ . Higher amounts of catalyst showed a slight positive effect on the degradation of CR. This could be explained in terms of availability of active sites on catalyst surface [34], light scattering and screening effect [35].

### 3.5. The effect of initial dye concentration on the decolorization of Congo Red

Influence of initial dye concentration on  $k_{app}$  values of the degradation of CR was studied at different concentrations varying from  $10 \text{ mg L}^{-1}$  to  $40 \text{ mg L}^{-1}$  in the presence of  $1.5 \text{ g L}^{-1}$  CS/n-CdS composite catalyst under simulated visible light. As shown in Fig. 12, the photodegradation rate depended on the initial concentration of CR. Correlation coefficient values ( $R^2$ ) decreased generally with increasing initial dye concentration. The result indicated that when the initial concentration of dye was lower, the correlation coefficient values ( $R^2$ ) were higher than 0.99, which was confirmed by the proposed kinetics for decolorization of CR in this process. On the other hand,  $k_{app}$  values of the dye degradation were observed to decrease with increasing initial dye concentration, which was in accordance with those reported in the literatures [36,37]. The ratio of degradation related to the probability of hydroxyl free radicals formation on the catalyst surface and to the probability of hydroxyl free radicals reacting with dye molecules [34]. As initial concen-

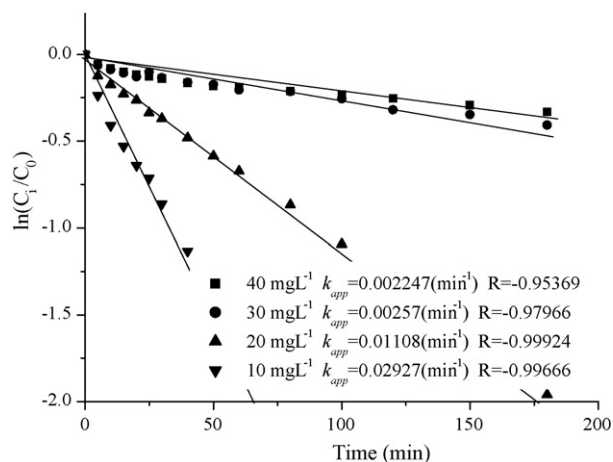


Fig. 12. Influence of initial dye concentration on the decolorization kinetics of CR.  $[C]_0 = 20 \text{ mg L}^{-1}$ ,  $[Cata.] = 1.5 \text{ g L}^{-1}$ , pH 6.0.

tration of the dye increased, the probability of reaction between dye molecules and oxidizing species also increased. On the contrary, the degradation ratio decreased with further increase in the dye concentration because the active sites on catalyst surface were covered by dye molecules. Another possible reason was that a high dye concentration shielded the visible light thus the light triggered catalysts decreased, thus concentration of hydroxyl free radicals decreased [38].

### 3.6. The effect of pH on the decolorization of Congo Red

The strong influence of pH value on CR photodegradation was performed as showed in Fig. 13. Natural pH of  $20 \text{ mg L}^{-1}$  CR is 6.0. The rate constants  $k_{app}$  as a function of pH value decreased in the order of  $6 > 8 > 10 > 12$ . The highest  $k_{app}$  value reached  $11.08 \times 10^{-3} \text{ min}^{-1}$  at pH 6 while the lowest  $k_{app}$  value was  $5.5 \times 10^{-3} \text{ min}^{-1}$  observed at pH 12. CR molecule with two sulfuric groups ionized easily even in acidic media and became a soluble CR anion [34]. At the same time, the residual amino groups of chitosan in CS/n-CdS were much more easily to be protonated at a low pH and could form electrostatic attraction to adsorb a quantity of dye anions [39]. Therefore, in the acidic solution, CR anions were easily adsorbed to CS/n-CdS with positive surface charge, while CR anions were generally excluded away from surface of catalyst at alkaline media. The CR anions could be oxidized more directly by hydroxyl radicals produced under visible light excitation in acidic

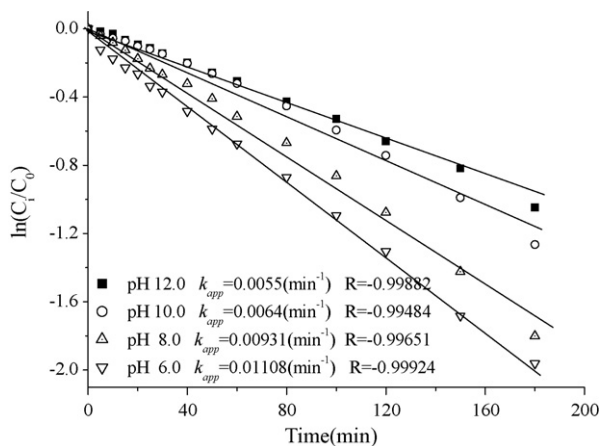


Fig. 13. Influence of initial pH on the decolorization kinetics of CR.  $[C]_0 = 20 \text{ mg L}^{-1}$ ,  $[Cata.] = 1.5 \text{ g L}^{-1}$ .

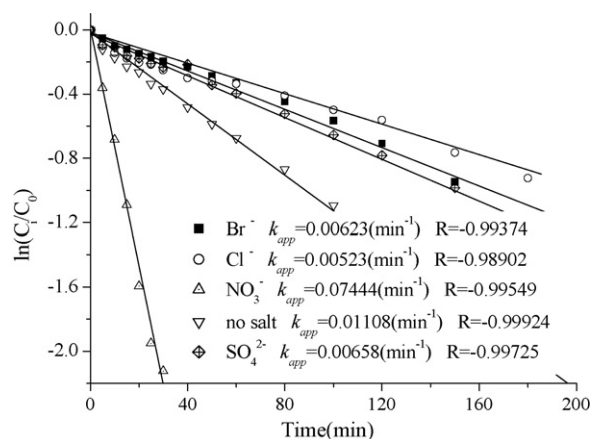
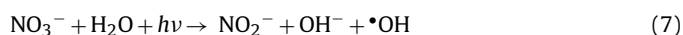


Fig. 14. Influence of co-existing anions on the decolorization rate of CR.  $[C]_0 = 20 \text{ mg L}^{-1}$ ,  $[Cata.] = 1.5 \text{ g L}^{-1}$ , pH 6.0.

media. That was why higher decolorization rate was obtained in acidic media.

### 3.7. The effect of co-existing anions on the decolorization of Congo Red

As we all know, there are large amounts of negative ions, such as  $\text{NO}_3^-$ ,  $\text{SO}_4^{2-}$ ,  $\text{Cl}^-$  and so on, in real wastewater produced by textile and dyestuff industries [34], of which great influence on photocatalytic decolorization and degradation of CR cannot be neglected. Because the effect of  $\text{Na}^+$  could be negligible [40],  $0.01 \text{ mol L}^{-1}$  corresponding sodium salts were separately added into the  $20 \text{ mg L}^{-1}$  CR solution and then carried out photocatalytic experiments under predetermined conditions. Fig. 14 shows the effects of some anions on the degradation of CR. Surprisingly, the presence of  $\text{NO}_3^-$  accelerated evidently the degradation reaction of CR, whereas the other chosen anions had an inhibitory effect on the decolorization of the dye. Addition of  $0.01 \text{ mol L}^{-1}$   $\text{NaNO}_3$  increased markedly the  $k_{app}$  value from  $11.08 \times 10^{-3} \text{ min}^{-1}$  to  $74.44 \times 10^{-3} \text{ min}^{-1}$ , while addition of  $0.01 \text{ mol L}^{-1}$   $\text{NaCl}$  decreased the  $k_{app}$  value to  $5.23 \times 10^{-3} \text{ min}^{-1}$ . Daneshaver et al. [41] and Epling and Lin [42] studied the effects of anionic species on degradation of dyes, and confirmed that  $\text{Cl}^-$  was a potent hydroxyl radical scavenging agent. Chang and Kuo [43] reported that  $\text{NO}_3^-$  possessed higher decolorization efficiency of some dye. The enhancement of decomposition rate by  $\text{NO}_3^-$  may be linked to the direct or indirect formation of hydroxyl radical chemically showed as following [44]:



### 3.8. Recycle of CS/n-CdS photocatalyst

For the purpose of practical implementation, it is essential to evaluate the stability and reuse of the catalyst. Fig. 15 shows the repetitive photodegradation of CR during five consecutive cycles with the same  $1.5 \text{ g L}^{-1}$  catalyst at  $20 \text{ mg L}^{-1}$  dye concentration, pH 6.0 and  $0.01 \text{ mol L}^{-1}$   $\text{NO}_3^-$  addition. After each cycle, the CS/n-CdS composite catalyst was washed with double distilled water and a fresh solution of CR was added before each photocatalytic run. The decolorization rates for the 5 cycling reuse were 93.6%, 86.6%, 86.3%, 84.4% and 82.7%, after 180 min of reaction time, respectively. The results showed that the catalytic activity of the catalyst had a slight decrease after first cycles. The reason may be the run off of the catalyst during washing and filtrating, and losing of adsorption ability of

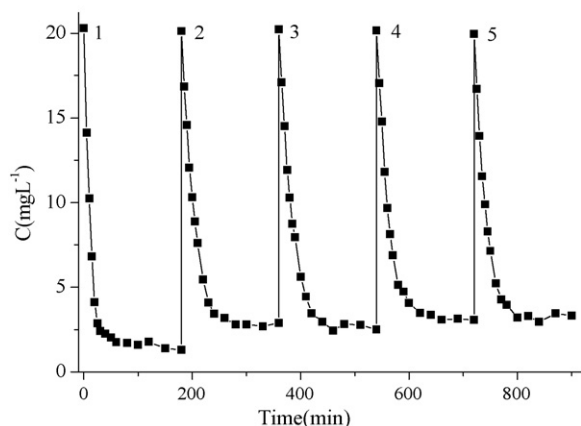


**Fig. 15.** Stability and recycle of CS/n-CdS.  $[C]_0 = 20 \text{ mg L}^{-1}$ ,  $[Cata.] = 1.5 \text{ g L}^{-1}$ , pH 6.0 and  $0.01 \text{ mol L}^{-1} \text{ NO}_3^-$  addition.

residual amino groups ( $-\text{NH}_2$ ) and hydroxyl ( $-\text{OH}$ ) in the chitosan. However, the decolorization efficiency kept relatively stable in the following repeated experiences, which confirmed that nano-CdS in the composite was combined steadily. From this point of view, the recycle of CS/n-CdS photocatalyst can confirm the relative stability of the CS/n-CdS composite.

#### 4. Conclusions

CS/n-CdS composite catalyst was prepared by simulating bio-mineralization process and could be efficiently applied for decolorization and degradation of the model compound (Congo Red). It has been found that the photocatalyst amount, initial dye concentration, the solution pH and the co-existing anions had strong influences on the decolorization and degradation of CR. The photocatalytic degradation kinetics of CR using CS/n-CdS under simulated visible light fitted the L–H kinetics model well. The dye could be more efficiently decolorized in acidic media than alkaline media. The presence of  $\text{NO}_3^-$  accelerated evidently the degradation reaction of CR. However, the other chosen anions ( $\text{Br}^-$ ,  $\text{SO}_4^{2-}$  and  $\text{Cl}^-$ ) had an inhibitory effect on the decolorization of the dye, of which the inhibitory effect of  $\text{Cl}^-$  was the most pronounced. It was found that 85.9% of degradation rate was achieved within 180 min of irradiation for  $20 \text{ mg L}^{-1}$  CR solution at natural pH of 6.0 in the presence of  $1.5 \text{ g L}^{-1}$  CS/n-CdS composite catalyst under simulated visible light. UV–vis spectra were analyzed to indicate that degradation of CR in the solution was the break up of the N=N bonds and degradation of aromatic fragment in this reaction system. The recycling experiments confirmed the relative stability of the catalyst.

#### Acknowledgements

The authors are grateful for the financial support of this research from the National Natural Science Foundation of China (No. 50808071). Special thanks to Mr. Changhua Ge and Mrs. Fang Wang for their assistance in this work.

#### References

- [1] N.M. Mahmoodi, M. Arami, N.Y. Limaee, N.S. Tabrizi, Decolorization and aromatic ring degradation kinetics of Direct Red 80 by UV oxidation in the presence of hydrogen peroxide utilizing  $\text{TiO}_2$  as a photocatalyst, *Chem. Eng. J.* 112 (2005) 191–196.
- [2] I.K. Konstantinou, T.A. Albanis,  $\text{TiO}_2$ -assisted photocatalytic degradation of azo dyes in aqueous solution: kinetic and mechanistic investigations: a review, *Appl. Catal. B: Environ.* 49 (2004) 1–14.
- [3] S. Papić, N. Koprivanac, A.L. Božić, A. Metić, Removal of some reactive dyes from synthetic wastewater by combined Al(III) coagulation/carbon adsorption process, *Dyes Pigments* 62 (2004) 291–298.
- [4] M. Özacar, İ.A. Şengil, Adsorption of reactive dyes on calcined alunite from aqueous solutions, *J. Hazard. Mater.* 98 (2003) 211–224.
- [5] G.M. Walker, L. Hansen, J.-A. Hanna, S.J. Allen, Kinetics of a reactive dye adsorption onto dolomitic sorbents, *Water Res.* 37 (2003) 2081–2089.
- [6] J. Sun, X. Wang, J. Sun, R. Sun, S. Sun, L. Qiao, Photocatalytic degradation and kinetics of Orange G using nano-sized Sn(IV)/ $\text{TiO}_2$ /AC photocatalyst, *J. Mol. Catal. A: Chem.* 260 (2006) 241–246.
- [7] Y. Cheng, H. Sun, W. Jin, N. Xu, Photocatalytic degradation of 4-chlorophenol with combustion synthesized  $\text{TiO}_2$  under visible light irradiation, *Chem. Eng. J.* 128 (2007) 127–133.
- [8] Z. Yu, H. Keppner, D. Laub, E. Mielczarski, J. Mielczarski, L.K. Minsker, A. Renken, J. Kiwi, Photocatalytic discoloration of Methyl orange on innovative parylene- $\text{TiO}_2$  flexible thin films under simulated sunlight, *Appl. Catal. B: Environ.* 79 (2008) 63–71.
- [9] A. Lu, Y. Li, M. Lv, C. Wang, L. Yang, J. Liu, Y. Wang, K. Wong, P. Wong, Photocatalytic oxidation of methyl orange by natural V-bearing rutile under visible light, *Sol. Energy Mater. Sol. Cells* 91 (2007) 1849–1855.
- [10] C. Wang, H. Shang, Y. Tao, T. Yuan, G. Zhang, Properties and morphology of CdS compounded  $\text{TiO}_2$  visible light photocatalytic nanofilm coated on glass surface, *Sep. Purif. Technol.* 32 (2003) 357–362.
- [11] H. Khallaf, I.O. Oladeji, L. Chow, Optimization of chemical bath deposited CdS thin films using nitrilotriacetic acid as a complexing agent, *Thin Solid Films* 516 (2008) 5967–5973.
- [12] J.C. Tristão, F. Magalhães, P. Corio, M. Terezinha, Electronic characterization and photocatalytic properties of CdS/ $\text{TiO}_2$  semiconductor composite, *J. Photochem. Photobiol. A: Chem.* 181 (2006) 152–157.
- [13] T. Kida, G. Guan, A. Yoshida,  $\text{LaMnO}_3$ /CdS nanocomposite: a new photocatalyst for hydrogen production from water under visible light irradiation, *Chem. Phys. Lett.* 371 (2003) 563–567.
- [14] L. Wu, J.C. Yu, X. Fu, Characterization and photocatalytic mechanism of nano-sized CdS coupled  $\text{TiO}_2$  nanocrystals under visible light irradiation, *J. Mol. Catal. A: Chem.* 244 (2006) 25–32.
- [15] P.R. Smith, J.D. Holmes, D.J. Richardson, D.A. Russell, J.R. Sodeau, Photophysical and photochemical characterization of bacterial semiconductor cadmium sulfide particles, *J. Chem. Soc., Faraday Trans.* 94 (1998) 1235–1241.
- [16] W.C.W. Chan, D.J. Maxwell, X. Gao, R.E. Bailey, M. Han, S. Nie, Luminescent quantum dots for multiplexed biological detection and imaging, *Curr. Opin. Biotechnol.* 13 (2002) 40–46.
- [17] N.V. Majeti, R. Kumar, A review of chitin and chitosan applications, *React. Funct. Polym.* 46 (2000) 1–27.
- [18] E. Guibal, Interactions of metal ions with chitosan-based sorbents: a review, *Sep. Purif. Technol.* 38 (2004) 43–74.
- [19] G.J. Coppello, F. Varela, R.M. Vivot, L.E. Díaz, Immobilized chitosan as biosorbent for the removal of Cd(II), Cr(III) and Cr(VI) from aqueous solutions, *Bioresour. Technol.* 99 (2008) 6538–6544.
- [20] X. Wang, Y. Du, S. Ding, L. Fan, X. Shi, Q. Wang, G. Xiong, Large two-photon absorbance of chitosan-ZnS quantum dots nanocomposite film, *Physica E* 30 (2006) 96–100.
- [21] Z. Li, Y. Du, Biomimic synthesis of CdS nanoparticles with enhanced luminescence, *Mater. Lett.* 57 (2003) 2480–2484.
- [22] J.Y. Chen, P.J. Zhou, J.L. Li, Y. Wang, Studies on the photocatalytic performance of cuprous oxide/chitosan nanocomposites activated by visible light, *Carbohydr. Polym.* 72 (2008) 128–132.
- [23] A. Webster, M.D. Halling, D.M. Grant, Metal complexation of chitosan and its glutaraldehyde cross-linked derivative, *Carbohydr. Res.* 342 (2007) 1189–1201.
- [24] H.Y. Chen, O. Zahraa, M. Bouchy, F. Thomas, J.Y. Bottero, Adsorption properties of  $\text{TiO}_2$  related to the photocatalytic degradation of organic contaminants in water, *J. Photochem. Photobiol. A: Chem.* 85 (1995) 179–186.
- [25] R.K. Wahi, W.W. Yu, Y. Liu, M.L. Mejia, J.C. Falkner, W. Nolte, V.L. Colvin, Photodegradation of Congo Red catalyzed by nanosized  $\text{TiO}_2$ , *J. Mol. Catal. A: Chem.* 242 (2005) 48–56.
- [26] S. Kaur, V. Singh,  $\text{TiO}_2$  mediated photocatalytic degradation studies of Reactive Red 198 by UV irradiation, *J. Hazard. Mater.* 141 (2007) 230–236.
- [27] W. Tan, A.K. Arof, FT-IR studies on interactions among components in hexanoyl chitosan-based polymer electrolytes, *Spectrochim. Acta A: Mol. Biomol. Spectrosc.* 63 (2006) 677–684.
- [28] J. Brugnerotto, J. Lizardi, F.M. Goycoolea, W.A. Monal, J. Desbrières, M. Rinaudo, An infrared investigation in relation with chitin and chitosan characterization, *Polymer* 42 (2001) 3569–3580.
- [29] Y. Kang, D. Kim, Enhanced optical sensing by carbon nanotube functionalized with CdS particles, *Sens. Actuators A: Phys.* 125 (2006) 114–117.
- [30] V. Singh, A. Tiwari, D.N. Tripathi, R. Sanghi, Microwave enhanced synthesis of chitosan-graft-polyacrylamide, *Polymer* 47 (2006) 254–260.
- [31] J. Wang, R.H. Li, Z.H. Zhang, W. Sun, R. Xu, Y.P. Xie, Z.Q. Xing, X.D. Zhang, Efficient photocatalytic degradation of organic dyes over titanium dioxide coating upconversion luminescence agent under visible and sunlight irradiation, *Appl. Catal. A: Gen.* 334 (2008) 227–233.
- [32] N.H. Ince, G. Tezcanlı, Reactive dyestuff degradation by combined sonolysis and ozonation, *Dyes Pigments* 49 (2001) 145–153.
- [33] Y. Iida, T. Kozuka, T. Tuziuti, K. Yasui, Sonochemically enhanced adsorption and degradation of methyl orange with activated aluminas, *Ultrasonics* 42 (2004) 635–639.

- [34] S. Erdemoğlu, S.K. Aksu, F. Sayılkan, B. İzgi, M. Asiltürk, H. Sayılkan, F. Frimmel, Ş. Güçer, Photocatalytic degradation of congo red by hydrothermally synthesized nanocrystalline TiO<sub>2</sub> and identification of degradation products by LC–MS, *J. Hazard. Mater.* 155 (2008) 469–476.
- [35] M. Huang, C. Xu, Z. Wu, Y. Huang, J. Lin, J. Wu, Photocatalytic decolorization of methyl orange solution by Pt modified TiO<sub>2</sub> loaded on natural zeolite, *Dyes Pigments* 77 (2008) 327–334.
- [36] A.P. Toor, A. Verma, C.K. Jotshi, P.K. Bajpai, V. Singh, Photocatalytic degradation of direct yellow 12 dye using UV/TiO<sub>2</sub> in a shallow pond slurry reactor, *Dyes Pigments* 68 (2006) 53–60.
- [37] B. Neppolian, M.V. Shankar, V. Murugesan, Semiconductor assisted photodegradation of textile dye, *J. Sci. Ind. Res.* 61 (2002) 224–230.
- [38] C.C. Liu, Y.H. Hsieh, P.F. Lai, C.H. Li, C.L. Kao, Photodegradation treatment of azo dye wastewater by UV/TiO<sub>2</sub> process, *Dyes Pigments* 68 (2006) 191–195.
- [39] H. Yoshida, A. Okamoto, T. Kataoka, Adsorption of acid dye on crosslinked chitosan fibers: equilibria, *Chem. Eng. Sci.* 48 (1993) 2267–2272.
- [40] A. Mohammad, K.C.L. Gary, W.M. Ralph, Effects of common inorganic anions on rates of photocatalytic oxidation of organic carbon over illuminated titanium dioxide, *J. Phys. Chem.* 94 (1990) 6820–6825.
- [41] N. Daneshavar, D. Salari, A.R. Khataee, Photocatalytic degradation of azo dye acid red 14 in water: investigation of the effect of operational parameters, *J. Photochem. Photobiol. A: Chem.* 157 (2003) 111–116.
- [42] G.A. Epling, C. Lin, Investigation of retardation effects on the titanium dioxide photodegradation system, *Chemosphere* 46 (2002) 937–944.
- [43] J.S. Chang, T.S. Kuo, Kinetics of bacterial decolorization of azo dye with *Escherichia coli* NO<sub>3</sub>, *Bioresour. Technol.* 75 (2000) 107–111.
- [44] R.G. Zepp, J. Hoigné, H. Bader, Nitrate-induced photooxidation of trace organic chemicals in water, *Environ. Sci. Technol.* 21 (1987) 443–450.